PHYSICAL REVIEW C **76**, 021902(R) (2007)

Initial fields and instabilities in the classical model of relativistic heavy-ion collisions

Kenji Fukushima
RIKEN BNL Research Center, Brookhaven National Laboratory, Upton, New York 11973, USA
(Received 22 May 2007; published 2 August 2007)

Color Glass Condensate (CGC) provides a classical description of dense gluon matter at high energies. Using the McLerran-Venugopalan (MV) model we calculate the initial energy density $\varepsilon(\tau)$ in the early stage of the relativistic nucleus-nucleus collision. Our analytical formula reproduces the quantitative results from lattice discretized simulations and leads to an estimate $\varepsilon(\tau = 0.1\ \mathrm{fm}) = 40 \sim 50\ \mathrm{GeV}\cdot\mathrm{fm}^{-3}$ in the (central) Au-Au collision at BNL Relativistic Heavy Ion Collider. We then formulate instabilities with respect to soft fluctuations that violate boost invariance inherent in hard CGC backgrounds. We find unstable modes arising, which are attributed to ensemble average over the initial CGC fields.

DOI: 10.1103/PhysRevC.76.021902 PACS number(s): 24.85.+p, 25.75.−q

In relativistic heavy-ion collisions, Color Glass Condensate (CGC) describes the initial state of the energetic gluon matter with the transverse momentum p_t up to the saturation scale Q_s, which universally characterizes the hadron or nucleus wave function in the small-x regime [1–10]. Given the scale Q_s at a certain value of Bjorken's x, the gluon distribution probed by processes with $Q^2 \ll Q_s^2$ is so dense that coherent fields should be more relevant than the individual particle picture during $\tau \lesssim Q_s^{-1}$. Physically Q_s^2 corresponds to the transverse density of partons and is estimated by the Golec-Biernat and Wüsthoff fit, $Q_s^2 = Q_0^2(x_0/x)^\lambda A^{1/3}$, where A is the atomic number. We can expect Q_s around $1 \sim 2$ GeV for the BNL Relativistic Heavy Ion Collider (RHIC) and around $2 \sim 3$ GeV for the Large Hadron Collider (LHC) in the case of $A = 197$ (Au-Au collision) assuming that relevant p_t is $\sim$1 GeV. This transient but still coherent gluon matter, which is often referred to as "Glasma" [7], should melt toward a quark-gluon plasma.

The physical property of Glasma has been mainly analyzed by numerical simulations in the lattice discretized formulation [4–9]. In this article we aim to approach Glasma in an analytical way along a line similar to that of the near-field expansion proposed by Fries, Kapusta, and Li [10]. The analytical method is desirable for a deeper insight into the Glasma, which presumably exists up to $\tau \lesssim Q_s^{-1} \sim 0.1$ fm in the Au-Au (central) collision at RHIC energy, $\sqrt{s} = 200$ GeV/nucleon, or even longer depending on the interpretation of the Glasma. In particular, the problem of *early thermalization* still has interesting unanswered questions [11]. We specifically address the following: is there any unstable mode growing around the initial CGC fields right after the collision? If any, it could speed up thermalization (or isotropization) even in the classical regime ($\tau \lesssim Q_s^{-1}$), besides non-Abelian plasma instabilities [12–15] which take place at later times. The pioneering numerical simulation [9] suggests the existence of "Glasma instability," though the literal time scale of instability seems to be greater than Q_s^{-1} by three orders of magnitude, probably because of the choice of tiny instability seeds. The delay in the instability onset has also been pointed out in the Hard Expanding Loop (HEL) approach to non-Abelian plasma instabilities [15].

We shall start with the boost-invariant CGC solution and estimate an initial energy density. It is convenient to adopt the Bjorken coordinates spanned by the proper time $\tau = \sqrt{t^2 - z^2}$ and the space-time rapidity $\eta = \frac{1}{2}\ln[(t+z)/(t-z)]$. The radial gauge $A_\tau = 0$ is understood throughout this work. The canonical momenta (chromoelectric fields) are read in this gauge as

$$E^i = \tau\partial_\tau A_i, \quad E^\eta = \tau^{-1}\partial_\tau A_\eta. \tag{1}$$

It should be mentioned that the metric is $g_{\tau\tau} = 1$, $g_{\eta\eta} = -\tau^2$, and $g_{xx} = g_{yy} = -1$ in accord with the convention in Refs. [9] and [16]. The equations of motion derived from Hamilton's equations lead us to

$$\partial_\tau E^i = \tau^{-1}D_\eta F_{\eta i} + \tau D_j F_{ji}, \quad \partial_\tau E^\eta = \tau^{-1}D_j F_{j\eta}. \tag{2}$$

These are the basic equations for the classical description valid in the early stage right after the collision. The initial condition is uniquely determined by boundary matching at singularities of the color sources $\rho^{(1)}(\boldsymbol{x}_\perp)\delta(x^-)$ and $\rho^{(2)}(\boldsymbol{x}_\perp)\delta(x^+)$, representing the propagation of Lorentz contracted nuclei [2,16], as follows,

$$\begin{aligned} A_{i(0)} &= \alpha_i^{(1)} + \alpha_i^{(2)}, \quad A_{\eta(0)} = 0, \\ E^i_{(0)} &= 0, \quad E^\eta_{(0)} = ig\left[\alpha_i^{(1)}, \alpha_i^{(2)}\right], \end{aligned} \tag{3}$$

where $\alpha_i^{(1)}$ and $\alpha_i^{(2)}$ are the gauge fields at $\tau < 0$ associated with the right-moving nucleus along the x^+ axis and the left-moving nucleus along the x^- axis [17]. It takes a pure-gauge form, $\alpha_i(\boldsymbol{x}_\perp) = -(1/ig)V(\boldsymbol{x}_\perp)\partial_i V^\dagger(\boldsymbol{x}_\perp)$, with the Wilson line defined by

$$V^\dagger(\boldsymbol{x}_\perp) = \mathcal{P}\exp\left[-ig\int dz^- \frac{1}{\boldsymbol{\partial}_\perp^2}\rho^{(1)}(\boldsymbol{x}_\perp)\delta(z^-)\right], \tag{4}$$

for $\alpha_i^{(1)}$. The Wilson line for $\alpha_i^{(2)}$ is given by replacement of x^- and $\rho^{(1)}(\boldsymbol{x}_\perp)$ by x^+ and $\rho^{(2)}(\boldsymbol{x}_\perp)$ in the above expression. We can compute the expectation values of physical observables by means of the average over the random color distribution inside nuclei using

$$\left\langle \rho_a^{(m)}(\boldsymbol{x}_\perp)\rho_b^{(n)}(\boldsymbol{y}_\perp)\right\rangle = g^2\mu^2\delta^{mn}\delta_{ab}\delta^{(2)}(\boldsymbol{x}_\perp - \boldsymbol{y}_\perp). \tag{5}$$

Here μ is the only dimensionful scale in the McLerran-Venugopalan (MV) model and related to the saturation scale Q_s. We later present all dimensionful quantities in μ.

Let us evaluate the initial energy density of the fields (3) at $\tau = 0$ with the color source average (5). To do this, we need to take an average of four Wilson lines $\langle V(\boldsymbol{x}_\perp)V^\dagger(\boldsymbol{y}_\perp)V(\boldsymbol{u}_\perp)V^\dagger(\boldsymbol{v}_\perp)\rangle$. We can find an algebraic technique in the Appendix of Ref. [18] and it is even possible to write a formal expression for more generic color structure [19]. After all, it turns out that the transverse fields are vanishing and that the longitudinal chromomagnetic fields, $B^\eta_{(0)} = F_{12(0)}$, are [8]

$$\frac{g^2}{(g^2\mu)^4}\cdot\left\langle 2\mathrm{tr}\left(B^\eta_{(0)}\right)^2\right\rangle = \frac{1}{32}N_c\left(N_c^2-1\right)\sigma^2. \tag{6}$$

The number of color is $N_c = 3$ in QCD. We defined σ resulting from the two-point function in terms of $\alpha_i^{(m)}$. To make a direct comparison to the numerical simulation transparently, we make use of the lattice regularization, which gives

$$\begin{aligned}\sigma &= \frac{1}{2L^2}\sum_{n_i=1-L/2a}^{L/2a}\frac{1}{2-\cos(2\pi n_1 a/L)-\cos(2\pi n_2 a/L)}\\ &\simeq \frac{1}{2\pi}\ln(cL/a).\end{aligned} \tag{7}$$

Here L is the size of the system fixed by $L^2 = \pi R_A^2$, and a is the lattice spacing. We got rid of the zero-mode $n_1 = n_2 = 0$ because of global neutrality. We numerically checked that the above logarithmic form adjusted by the constant $c \simeq 1.36$ is a quite good approximation. Some further calculations end up with the same amount of the chromoelectric field squared; $\langle 2\mathrm{tr}(E^\eta_{(0)})^2\rangle = \langle 2\mathrm{tr}(B^\eta_{(0)})^2\rangle$. As a result, we can estimate the initial energy density as

$$\frac{g^2}{(g^2\mu)^4}\cdot\varepsilon_{(0)} = \frac{3}{4}\sigma^2, \tag{8}$$

with $N_c = 3$ substituted. This a and L dependent result should be interpreted carefully, while the quantitative output somehow agrees with the latest simulation by Lappi; our estimates using Eqs. (7) and (8) yields 0.81 and 0.90 for $L/a = 500$ and 700, which are close to the values of 0.76 and 0.88 reported in Ref. [8]. The logarithmic singularity has also been found in Refs. [8] and [10]. The singularity arises from the approximations in which we regarded the colliding nuclei as infinitely thin in the longitudinal direction and in which the random color distribution is uncorrelated at arbitrary microscopic scale in transverse space.

Next, we step away from the singularity located at $\tau = 0$ by the near-field expansion in terms of τ, i.e., $\mathcal{O} = \mathcal{O}_{(0)} + \mathcal{O}_{(1)}\tau + \mathcal{O}_{(2)}\tau^2 + \cdots$. The first-order corrections are vanishing, and the second-order fields are

$$\begin{aligned}A_{i(2)} &= \tfrac{1}{2}E^i_{(2)} = \tfrac{1}{4}D_{j(0)}F_{ji(0)},\\ A_{\eta(2)} &= \tfrac{1}{2}E^\eta_{(0)}, \quad E^\eta_{(2)} = \tfrac{1}{2}D_{j(0)}F_{j\eta(2)},\end{aligned} \tag{9}$$

where

$$\begin{aligned}F_{ji(0)} &= -ig\left(\left[\alpha_j^{(1)},\alpha_i^{(2)}\right]+\left[\alpha_j^{(2)},\alpha_i^{(1)}\right]\right),\\ F_{j\eta(2)} &= \tfrac{1}{2}D_{j(0)}E^\eta_{(0)},\end{aligned} \tag{10}$$

which physically represent the initial longitudinal and second-order transverse chromomagnetic fields.

Using these expressions we calculate the contributions to the energy density of order τ^2 to find the same amount of chromomagnetic and chromoelectric fields again. Because the initial state has nonzero longitudinal fields, it follows that the cross terms between the zeroth and second-order terms give

$$\begin{aligned}&\frac{g^2}{(g^2\mu)^4}\cdot 2\left\langle 2\mathrm{tr}(B^\eta_{(2)}B^\eta_{(0)})\right\rangle\\ &\quad= \frac{g^2}{(g^2\mu)^4}\cdot 2\left\langle 2\mathrm{tr}(E^\eta_{(2)}E^\eta_{(0)})\right\rangle\\ &\quad= -\frac{1}{32}N_c\left(N_c^2-1\right)\sigma\cdot\chi+\mathcal{O}(\sigma^3),\end{aligned} \tag{11}$$

where we defined

$$\chi = \frac{1}{L^2}\sum_{n_i=1-L/2a}^{L/2a} \simeq \frac{1}{a^2}. \tag{12}$$

We dropped terms proportional to σ^3 not containing χ because $\chi \gg \sigma$ when a is small. In the same approximation the transverse fields of order τ^4 (that is, τ^2 order in the energy density) result in

$$\begin{aligned}\frac{g^2}{(g^2\mu)^4}\cdot\left\langle 2\mathrm{tr}\left(B^i_{(2)}B^i_{(2)}\right)\right\rangle &= \frac{g^2}{(g^2\mu)^4}\cdot\left\langle 2\mathrm{tr}\left(E^i_{(2)}E^i_{(2)}\right)\right\rangle\\ &= \frac{1}{64}N_c\left(N_c^2-1\right)\sigma\cdot\chi+\mathcal{O}(\sigma^3).\end{aligned} \tag{13}$$

Then we get the expanded series

$$\begin{aligned}\frac{g^2}{(g^2\mu)^4}\cdot\varepsilon &\simeq \frac{g^2}{(g^2\mu)^4}[\varepsilon_{(0)}+\varepsilon_{(2)}\tau^2]\\ &= \frac{1}{32}N_c\left(N_c^2-1\right)\sigma\left[\sigma-\pi\frac{(g^2\mu\tau)^2}{(g^2\mu a)^2}\right].\end{aligned} \tag{14}$$

It is obvious from Eq. (14) that the τ expansion behaves badly for small values of a, which is also clear from the dotted curve in Fig. 1 that plots Eq. (14).

The naive τ expansion is, in fact, ill-defined. This is because, as pointed out in Ref. [7], the energy density behaves as $\sim(\ln\tau)^2$ near $\tau = 0$ when the colliding nuclei are infinitely thin. Therefore, the naive Taylor expansion around $\tau = 0$ is meaningless. Nevertheless, we stress that we can derive meaningful information from Eq. (14); we know that the asymptotic form is $\sim(\ln\tau)^2$ in the $a \to 0$ limit and we also know that the regularized expansion is $\sim c_1\ln(L/a)[\ln(L/a)+c_2(\tau/a)^2]$ with a kept finite. The simplest analytical function satisfying these two requirements is $\sim c_1\{\ln[L^2/(a^2-c_2\tau^2)]\}^2$, which means

$$\frac{g^2}{(g^2\mu)^4}\cdot\varepsilon \simeq \frac{3}{4}\left\{\frac{1}{4\pi}\ln\left[\frac{c^2(g^2\mu L)^2}{(g^2\mu a)^2+\pi(g^2\mu\tau)^2}\right]\right\}^2. \tag{15}$$

The comparison to data obtained in the numerical simulation is presented in Fig. 1. This simple log-ansatz works well as long

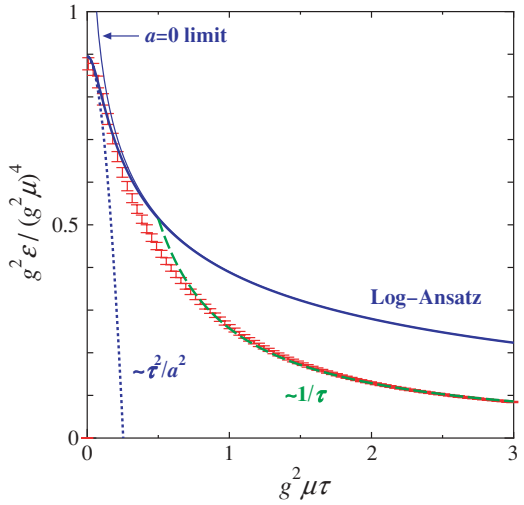

FIG. 1. (Color online) Comparison of the energy density in the case of $L/a = 700$; the data with error bars are taken from Ref. [8]. The dotted and solid curves represent the naive expansion in Eq. (14) and the log-ansatz in Eq. (15), respectively. The dashed curve scales as $1/\tau$, the starting point of which is chosen at $g^2\mu\tau = 0.5$, meaning that the "formation time" [4] is $g^2\mu\tau_D \sim 0.5$.

as $g^2\mu\tau \lesssim 0.5$ and is stable under the $a \to 0$ limit as shown by a thin curve in the figure.

So far, we reached an ansatz (15) with the infrared cutoff provided by the nucleus size L in a heuristic way. In reality, however, the long-ranged correlation should be cut off by the confining scale $\sim\Lambda_{\rm QCD}^{-1}$ rather than L. In the continuum limit, hence, the initial energy density in the central collision at $\tau \ll (g^2\mu)^{-1}$ should be estimated by

$$\varepsilon = \frac{3}{16\pi^2 g^2}(g^2\mu)^4\left\{\ln\left(\Lambda_{\rm QCD}^{-1}/\tau\right)\right\}^2. \tag{16}$$

In writing Eq. (16) we put the constants c and π appearing in Eq. (15) away into the ambiguity of $\Lambda_{\rm QCD}$. We remark that the $\Lambda_{\rm QCD}$ dependence would be milder than the above in the regime after the "formation time" as investigated in Ref. [4].

It is interesting to apply our formula (16) to the Au-Au collision at RHIC in the physical unit. We make use of the parameter choice as commonly used in the numerical simulation, i.e., $g^2/4\pi = 1/\pi$ and $g^2\mu = 2$ GeV [4–6,10]. As for the confining scale, we vary $\Lambda_{\rm QCD}^{-1}$ from 1 fm to 12 fm $\simeq L$. The results are summarized in the following table.

Our log-ansatz overestimates the energy density and the third row shows the corrected values with a factor 0.67 inferred from Fig. 1. This factor might depend on $\Lambda_{\rm QCD}^{-1}$, and, thus, the numbers listed in the second and third rows should be considered as the upper and lower bounds.

It is a natural choice to take the confining scale as the nucleon size $\sim$1fm; the estimate of the initial energy density is then $\varepsilon(\tau = 0.1\ \text{fm}) = 40 \sim 50\ \text{GeV}\cdot\ \text{fm}^{-3}$. This value is significantly smaller than the previous estimates, 130 GeV $\cdot$ fm^{-3} in Ref. [8] and 260 GeV $\cdot$ fm^{-3} in Ref. [10], reflecting difference between the choices $\Lambda_{\rm QCD}^{-1} = 1$ fm and $\Lambda_{\rm QCD}^{-1} = L \sim 12$ fm, but is rather consistent with the simulation with color neutrality of finite nuclei taken into account [5] that found $\epsilon(\tau = \tau_D \simeq 0.3\ \text{fm}) = 7.1 \sim 40\ \text{GeV}\cdot\ \text{fm}^{-3}$.

TABLE I.

$\Lambda_{\rm QCD}^{-1}$ [fm]	1	3	5	8	10	12
$\varepsilon(\tau = 0.1\ \text{fm})$ [GeV $\cdot$ fm^{-3}]	53	115	152	191	211	228
Corrected [GeV $\cdot$ fm^{-3}]	36	77	102	128	142	153

When $g^2\mu\tau$ becomes larger, the energy density comes to scale as $\sim\tau_0/\tau$ because of (almost free streaming) longitudinal expansion [9,11]. It should be noted that the scaling law in the classical regime is different from the (one-dimensional) hydrodynamic one, $\epsilon(\tau) \propto (\tau_0/\tau)^{4/3}$. For reference we plot the scaling behavior $\varepsilon(\tau)/\varepsilon(\tau_0) = \tau_0/\tau$ in Fig. 1 indicated by the dashed curve with a choice of $g^2\mu\tau_0 = 0.5$. The expanding system at late times is dilute so that this scaling behavior is to be justified by the solution of Eq. (2) in the weak field limit, which in fact scales as [2,8]

$$A_i \sim A_\eta \sim 1/\sqrt{\tau}. \tag{17}$$

The energy density is dominated only by the Abelian part $\propto(\partial A)^2$; hence it follows the τ_0/τ scaling. We note a curious observation that, if we extrapolate our estimate $\varepsilon(\tau = 0.1\ \text{fm})$ up to $\tau = 1$ fm assuming the τ_0/τ scaling, the initial energy density obtained accordingly is very close to the standard estimate by means of the Bjorken formula: $\epsilon(\tau = 1\ \text{fm}) \sim 5.1\ \text{GeV}\cdot\ \text{fm}^{-3}$.

For the remainder of this article, we consider the problem of instability. We treat fluctuations δA_i and δE^i in the linear order around the boost-invariant CGC background that we discuss above. As formulated in Ref. [16], δE^η should be constrained by the Gauss law and we drop δA_η because it is accompanied by τ^2 from the metric. In what follows we regard η-dependent fluctuations, δA_i and δE^i, as the "soft" fields and η-independent CGC fields as the "hard" background that brings about instability. The linearized equations of motion are

$$\begin{aligned}\tau\partial_\tau\delta\tilde{A}_i &= \delta\tilde{E}^i,\\ \partial_\tau\delta\tilde{E}^i &= -\tau^{-1}\nu^2\delta\tilde{A}_i + \tau G_{ij}^{-1}\delta\tilde{A}_j,\end{aligned} \tag{18}$$

where we introduce the Fourier transform $\delta\tilde{A}_i$ from η to the wave number ν (i.e., $\partial_\eta^2\delta A_i(\eta) \to -\nu^2\delta\tilde{A}_i(\nu)$) and we denote the inverse of the transverse background gluon propagator as G_{ij}^{-1} whose definition is

$$G_{ij}^{-1ab} = \delta_{ij}(D_kD_k)^{ab} - (D_iD_j)^{ab} + 2gf^{\rm acb}F_{ij}^c. \tag{19}$$

We note that, in correspondence with the HEL approach, the color current encoding the anisotropic distribution of hard background is identified as $j_i^a = [G_{ij}^{-1ab} - \delta^{ab}(\delta_{ij}\partial_k\partial_k - \partial_i\partial_j)]\delta\tilde{A}_j^b$. Although it is not clear whether this current could have anything to do with that in the HEL approach after the ensemble average, we can shortly confirm that instability may occur even in the purely classical regime.

It is easy to solve Eq. (18) to obtain $\delta\tilde{A}_i$ as a function of a given constant CGC background, $G_{(0)}^{-1}$ at initial time, because we can diagonalize $G_{(0)}^{-1}$ in a proper basis of $\delta\tilde{A}_i$. If we write its eigenvalues as λ, the solution is

$$\delta\tilde{A}_i(\lambda) = c_{1i}{\rm Re}I_{i\nu}(\sqrt{\lambda}\tau) + c_{2i}{\rm Im}I_{i\nu}(\sqrt{\lambda}\tau), \tag{20}$$

for $\lambda > 0$ (which exponentially grows), and

$$\delta\tilde{A}_i(\lambda) = c_{1i}\mathrm{Re}J_{i\nu}(\sqrt{|\lambda|}\tau) + c_{2i}\mathrm{Im}J_{i\nu}(\sqrt{|\lambda|}\tau), \qquad (21)$$

for $\lambda < 0$ (which oscillatorily diminishes), where $J_n(x)$ and $I_n(x)$ are the first-kind and modified Bessel functions. These special functions are singular as $(\sqrt{|\lambda|}\tau)^{\pm i\nu}$, which furiously rotates in complex space as $\tau \to 0$. At a later time when the asymptotic behavior (17) realizes due to expansion, λ is no longer a constant but a function of time like $\sim \xi/\tau$ with some dimensionful constant ξ, which results in the solutions $I_{2\pm i\nu}(2\sqrt{\xi\tau})$ for $\xi > 0$ and $J_{2\pm i\nu}(2\sqrt{|\xi|\tau})$ for $\xi < 0$. For other general cases, the τ dependence in the eigenvalue is intricate, and one needs to solve Eq. (18) numerically.

We do not treat such a general case but what we pursue here is to clarify whether the *initial* CGC fields could induce exponential growth for soft degrees of freedom. We consider this because the initial CGC configurations at $\tau = 0$ are the most (spatially) anisotropic (namely, large longitudinal and zero transverse fields) and thus anticipated to cause the most unstable modes. Under such extreme circumstances we expect that the physics of instability becomes clear. Thus, as a first trial, it should be an appropriate starting point. We can say that what we will do is to extract the *tendency* toward instability under the presence of the CGC background. For simplicity we focus on the case where fluctuations are uniform in transverse space, i.e., $\partial_i\delta\tilde{A} = 0$, which should be the most unstable, as adopted in Ref. [15].

We should calculate the Gaussian average (5) of the transverse chromomagnetic field $\langle(B_i)^2\rangle \simeq \langle(\nu\delta\tilde{A}_i)^2\rangle$ and the chromoelectric field $\langle(E_i)^2\rangle \simeq \langle(\tau\partial_\tau\delta\tilde{A}_i)^2\rangle$, which were as small as $\sim\tau^4$ previously but nonzero this time with fluctuations depending on η, contributing to the longitudinal pressure [9]. The straightforward calculation is, however, technically hard. We approximately do it by picking up the mean value,

$$\left\langle G^{-1ab}_{(0)ij}\right\rangle = \delta_{ij}\delta^{ab}\bar{\lambda} = -\delta_{ij}\delta^{ab}\tfrac{3}{8}\sigma(g^2\mu)^2, \qquad (22)$$

where σ is defined in Eq. (7), and taking the ensemble average over its dispersion,

$$\left\langle G^{-1ac}_{(0)ik}G^{-1cb}_{(0)kj}\right\rangle - \delta_{ij}\delta^{ab}\bar{\lambda}^2 = \delta_{ij}\delta^{ab}\delta\lambda^2 = \delta_{ij}\delta^{ab}\tfrac{3}{8}\chi(g^2\mu)^2, \qquad (23)$$

where χ is defined in Eq. (12).

Because $\bar{\lambda}$ is negative, the soft fluctuations in the vicinity of the averaged CGC background are stable, belonging to the type of solution (21). The eigenvalue of $G^{-1}_{(0)}$ distributes according to random CGC configurations and spreads from $\bar{\lambda}$ with the dispersion $\delta\lambda$, meaning that some CGC configurations may have negative λ. That is, if we evaluate

$$\langle\mathcal{O}[\delta\tilde{A}(\lambda)]\rangle \simeq \int_{-\infty}^{\infty} d\lambda\mathcal{O}[\delta\tilde{A}(\lambda)]e^{-(\lambda-\bar{\lambda})^2/2\delta\lambda^2}, \qquad (24)$$

using Eq. (20), the contributions near $\lambda \simeq \bar{\lambda}$ dominate only when time is small until the negative λ constituents grow up as time elapses. The transverse field strengths obtained in this way are plotted in Fig. 2.

To draw Fig. 2, we chose the initial time $g^2\mu\tau_0 = 0.001$ at which we set c_1 and c_2 of Eq. (20) or Eq. (21) by the initial condition, $\delta\tilde{A}_i = c/\sqrt{\nu}$ and $\delta\tilde{E}_i = \tau_0\partial_\tau\delta\tilde{A}_i = c\sqrt{\nu}$, inspired by quantum fluctuations discussed in Ref. [16]. It is interesting to see that this specific initial condition ($\delta\tilde{E}_i \sim \nu\delta\tilde{A}_i$) makes $\langle(B_i)^2\rangle \simeq \langle(\nu\delta\tilde{A}_i)^2\rangle$ and $\langle(E_i)^2\rangle$ comparable to each other, leading to their almost alternate oscillations. That is why the sum of transverse field strengths depicted in Fig. 2 never comes close to zero, which is in contrast to the results in Ref. [15].

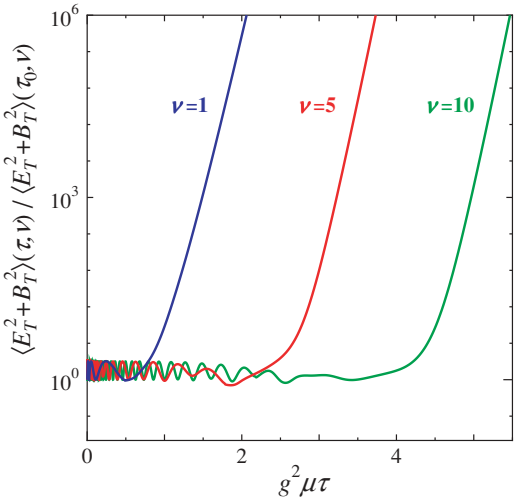

FIG. 2. (Color online) Instability tendency with the initial CGC background fixed at $\tau = 0$ in the case of $L/a = 700$ for different wave numbers $\nu = 1$, 5, and 10 from the left to the right.

We can conclude that there is certainly a tendency toward instability associated with the initial CGC background. The onset of instability in the present case is located much earlier than in preceding works. It is because we only investigated the strongest instability encompassed in the initial CGC fields. Because the CGC background itself evolves with time, in fact, the genuine growth of instability should be slower and weaker than shown in Fig. 2. Nevertheless, we can learn the qualitative character of the "Glasma" instability. The intuitive picture is as follows. The soft fluctuations of gluon fields are non-Abelian charged and feel a force under influence from the CGC background. The ensemble of random CGC distribution contains not only color fields that suppress the color current provided by charged soft fluctuations but also color fields that amplify the current. Although the current is suppressed on average, the large τ behavior is predominantly determined by the mixture of CGC fields that enhance the input current. Therefore, we think that it is a rare fluctuation in the CGC ensemble from which the Glasma instability can occur.

It is necessary to deal with $\lambda(\tau)$ not as a constant but rather as a function of τ to quantify instability further. In our treatment mentioned above we dropped the effect of longitudinal expansion for the hard part, while the exponential growth should take the form of $I_{2\pm i\nu}(2\sqrt{\xi\tau}) \sim \tau^{-1/2}\exp[2\sqrt{\xi\tau}]$ asymptotically when $\lambda \sim \xi/\tau$, as we remarked before. The analytical estimate of ξ deserves future clarification. Also, we must evaluate $\bar{\lambda}$ and $\delta\lambda$ in a resummed form like Eq. (15) beyond the naive expressions Eqs. (22) and (23). As a matter of fact, the growth rate seems to be determined by $\bar{\lambda}$ and $\delta\lambda$ regardless of ν in view of our results in Fig. 2. Quantitative details of an analytical description should be

improved with guided systematic instability studies in the numerical simulation in the future.

In summary, we developed an analytic formula to estimate the initial energy density. Our conclusion is $\epsilon(\tau = 0.1\ \mathrm{fm}) = 40 \sim 50\ \mathrm{GeV} \cdot\ \mathrm{fm}^{-3}$ in the (central) Au-Au collision at RHIC. The uncertainty comes from the infrared cutoff (or confining) scale. Also, we analyzed the tendency toward instability in the presence of the initial CGC background fixed at $\tau = 0$. We found that unstable modes exist as a result of the ensemble average of random CGC configurations, some of which strengthen the color current brought in by soft fluctuations. Although the Glasma instability might have a connection to non-Abelian plasma instabilities at a deeper level, we emphasize that we could understand the Glasma instability not relying on the picture of plasma instabilities that are premised on anisotropic momentum distribution of hard particles. The bottom line is, thus, that the Glasma instability exists from $\tau = 0$ even when the particle picture is irrelevant.

The author thanks Larry McLerran, Raju Venugopalan, Tuomas Lappi, Kazu Itakura, and Yuri Kovchegov for useful discussions. He is especially grateful to Tuomas Lappi for sending him the simulation data and to Raju Venugopalan for helpful comments on the manuscript. This work was supported by RIKEN BNL Research Center and the U.S. Department of Energy under Cooperative Research Agreement DE-AC02-98CH10886.

[1] L. D. McLerran and R. Venugopalan, Phys. Rev. D **49**, 2233 (1994); **49**, 3352 (1994); **50**, 2225 (1994).
[2] A. Kovner, L. D. McLerran, and H. Weigert, Phys. Rev. D **52**, 3809 (1995); **52**, 6231 (1995).
[3] Y. V. Kovchegov and D. H. Rischke, Phys. Rev. C **56**, 1084 (1997).
[4] A. Krasnitz and R. Venugopalan, Nucl. Phys. **B557**, 237 (1999); Phys. Rev. Lett. **84**, 4309 (2000); **86**, 1717 (2001).
[5] A. Krasnitz, Y. Nara, and R. Venugopalan, Phys. Rev. Lett. **87**, 192302 (2001); Nucl. Phys. **A717**, 268 (2003); **A727**, 427 (2003).
[6] T. Lappi, Phys. Rev. C **67**, 054903 (2003).
[7] T. Lappi and L. McLerran, Nucl. Phys. **A772**, 200 (2006).
[8] T. Lappi, Phys. Lett. **B643**, 11 (2006).
[9] P. Romatschke and R. Venugopalan, Phys. Rev. Lett. **96**, 062302 (2006) [arXiv:hep-ph/0510121]; Phys. Rev. D **74**, 045011 (2006) [arXiv:hep-ph/0605045].
[10] R. J. Fries, J. I. Kapusta, and Y. Li, arXiv:nucl-th/0604054.
[11] Y. V. Kovchegov, Nucl. Phys. **A762**, 298 (2005); **A764**, 476 (2006).
[12] S. Mrowczynski, Phys. Lett. **B214**, 587 (1988); **B314**, 118 (1993); **B393**, 26 (1997).
[13] S. Mrowczynski, A. Rebhan, and M. Strickland, Phys. Rev. D **70**, 025004 (2004).
[14] P. Arnold, J. Lenaghan, and G. D. Moore, JHEP 08 (2003) 002; P. Arnold, J. Lenaghan, G. D. Moore, and L. G. Yaffe, Phys. Rev. Lett. **94**, 072302 (2005); P. Arnold, G. D. Moore, and L. G. Yaffe, Phys. Rev. D **72**, 054003 (2005); A. Rebhan, P. Romatschke, and M. Strickland, Phys. Rev. Lett. **94**, 102303 (2005); JHEP 09 (2005) 041; D. Bodeker, JHEP 10 (2005) 092; P. Arnold and G. D. Moore, Phys. Rev. D **73**, 025006 (2006).
[15] P. Romatschke and A. Rebhan, Phys. Rev. Lett. **97**, 252301 (2006).
[16] K. Fukushima, F. Gelis, and L. McLerran, Nucl. Phys. **A786**, 107 (2007).
[17] Y. V. Kovchegov, Phys. Rev. D **54**, 5463 (1996).
[18] J. P. Blaizot, F. Gelis, and R. Venugopalan, Nucl. Phys. **A743**, 57 (2004).
[19] K. Fukushima and Y. Hidaka, JHEP 06 (2007) 040.